GeoAmericas2020
4th PAN AMERICAN CONFERENCE ON GEOSYNTHETICS
26-29 APRIL 2020 • RIO DE JANEIRO • BRAZIL

Effects of Slope Inclinations, Loading Conditions, and Geotextile Lengths on Geotextile-Reinforced Earth Wall Behavior

H. Oh, Department of Civil and Environmental Engineering, University of Wisconsin-Madison, Madison, WI, USA

ABSTRACT
This study conducted laboratory tests to evaluate effects of slope inclinations, loading condition, and geotextile lengths on geotextile-reinforced earth wall (GREW) that consists of non-woven polypropylene geotextile fabrics and re-bar mesh nets. In the experimental tests, horizontal displacements under three cumulative loading conditions of 50 kPa, 100 kPa, and 250 kPa were measured using 5 linear variable differential transformers (LVDTs). Three slope gradients (73.3°, 59°, and 45°) and geotextile lengths (0 cm, 10 cm, 14 cm, and 20 cm) were applied to investigate how the displacements changed. The results show that maximum horizontal displacements were observed near the top surface when the slope inclination was 45° while those were measured around middle of slopes when the inclinations were 73.3° and 59°. As the loading condition and the inclination increased from 50 kPa to 250 kPa and from 45° to 73.3°, respectively, or the length of geotextiles decreased from 20 cm to 0 cm, maximum horizontal displacements increased. In comparisons of the maximum horizontal displacements for non-reinforced wall and GREW, maximum horizontal displacements decreased by 60.3% with the reinforcements. These results imply that GREW can be stabilized with a decrease in the slope inclination and/or increase in the geotextile length. This study expands on a limited experimental database and thus provide empirical backgrounds for more precise GREW design.

1. INTRODUCTION

Geotextile is a polymer-based fabric and typically classified into two types in terms of its structures: woven and non-woven. Weaving structure of woven geotextile provides a relatively higher load capacity with a low permeability, while mechanically entangled fiber structure of non-woven geotextile has a relatively lower load capacity with a high permeability. Both woven and non-woven geotextiles are durable, flexible, cost-effective, and easy handling, and accordingly the geotextiles have been broadly used as reinforcements for various mechanically stabilized earth (MSE) retaining structures (e.g., geotextile-reinforced earth wall (GREW), roads, bridge abutments, embankments). For example, interactions of the soil and geotextile in GREW improve friction and adhesion of the soil at the interface. The improved soil friction and adhesion increase a resistance to loads, such as soil self-weight, applied surcharges, and seismic loading (Leshchinsky, 1985; Juran and Christopher, 1989; Claybourn and Wu, 1993; Al Hattamleh and Muhunthan, 2006; Benjamim et al., 2007).

Experimental research on evaluating GREW has been extensively performed at laboratory and field scales. In laboratory testing, soil deformations were measured using linear variable differential transformers (LVDTs) once a loading is applied on top surface of the soil (Juran and Christopher, 1989; Porbaha and Goodings, 1996; Chen et al., 2007; Viswanadham and König, 2009; Portelinha et al., 2012). Behavior of GREW was significantly dependent on geotextile properties, such as extensibility, spacing, and length, as well as soil physical properties. According to Juran and Christopher (1989), facing displacement of GREW greatly decreases as extensible reinforcements (e.g., geotextiles, geogrids) are replaced with metallic reinforcements. Chen et al. (2007) described that decreasing the reinforcement spacing is more effective than increasing the reinforcement length to reduce wall deformation. There also exists a critical reinforcement length; there is no more benefit when the reinforcement is longer than the critical length. Long-term displacements of GREW at a field site has also evaluated by previous researchers (e.g., Bakeer et al., 1998; Benjamim et al., 2007; Portelinha et al., 2013; Portelinha et al., 2014). Findings obtained from field monitoring indicate that there are no significant displacements under precipitation (Portelinha et al., 2013). Portelinha et al. (2014) also demonstrated that performance of non-woven GREW is equivalent to woven GREW performance even after intense precipitation periods. In addition to experimental studies, GREW behavior has numerically analyzed using a finite element method (Lee and Manjunath, 2000; Rowe and Skinner, 2001; Hatami and Bathurst, 2005; Al Hattamleh and Muhunthan, 2006). The previous studies compared wall deformations and reinforcement strains obtained from experiments and numerical analyses, and the observed results and predicted results are well aligned in their analyses.

Despite of the previous studies on GREW, there are still limited experimental studies that investigate behavior of GREW under various conditions. For example, majority of the previous studies (e.g., Juran and Christopher, 1989; Chen et al., 2007; Portelinha et al., 2012) evaluated GREW behavior at 90 º gradient under a constant loading. The objective of this study is thus to experimentally investigate how GREW behaves under various inclinations, loading conditions, and geotextile lengths.

2. MATERIALS AND METHODS

For laboratory testing, soil sample was collected from a field site and classified as silty sand (SM) by ASTM D422 and ASTM D2487. Cohesion (c) and friction angle (ϕ) of the soil were measured by direct shear test (ASTM D3080). Compaction test using standard effort (ASTM D698) was also performed to investigate maximum dry unit weight (γ_{dmax}) and optimum water content (w_{opt}). Table 1 summarizes the soil physical properties.

Table 1. Physical properties of the soil specimen.

Soil Type	D_{50} (mm)	Fines (%)	G_s	c (kPa)	ϕ (°)	γ_{dmax} (kN/m^3)	w_{opt} (%)
Silty Sand (SM)	0.25	28.4	2.66	20.59	34.8	18.44	12.9

Laboratory apparatus includes a model chamber (length = 1.6 m, width = 0.5, height = 1 m), a load cell, a load plate, 5 LVDTs, non-woven geotextiles, and re-bar reinforcements [Figure 1(a) and (b)]. Front of the model chamber consisted of high strength acrylic plate (thickness = 1 cm) to visually observe slope displacements and failures. On bottom of the chamber, foundation was made using concrete (concrete compressive strength = 22.5 MPa), and cohesion and friction angle between the soil and foundation were 10.79 kPa and 38°, respectively. Since experimental settings in this study were modeling a typical field site with downscale of about 1/20, non-woven geotextiles, which have relatively lower load capacities, were used for reinforcements. The geotextile properties were as follows: 1) length = 50cm, 2) width = 20 cm, 3) thickness = 0.54 mm, 4) density = 0.09 kg/m^3, 5) tensile strength = 2.65 kN/m, and 6) strain = 25 %. Cohesion and friction angle between the soil and geotextile were 22.56 kPa and 35.2°, respectively. In addition to the geotextiles, re-bar reinforcements that consist of steel wires (diameter = 2 mm) were used to model facing elements.

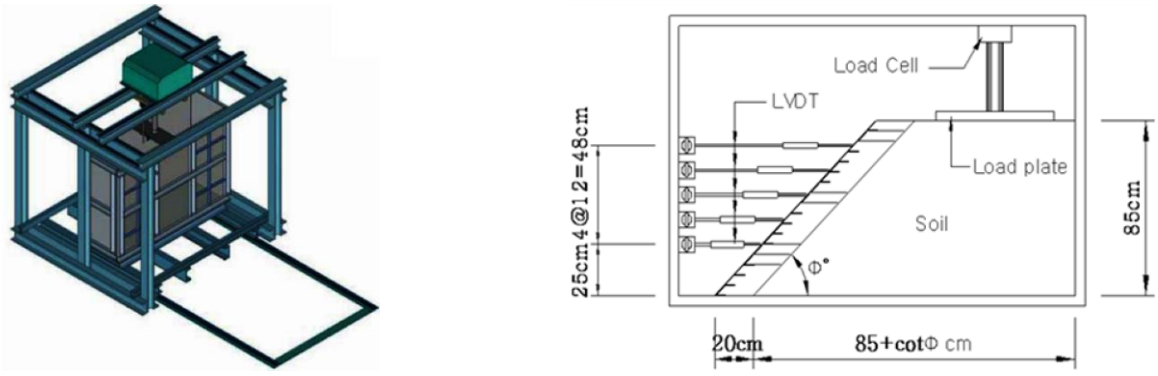

(a) 3-D schematic diagram of model setup (b) Model cross-section and configuration of instrumentations

Figure 1. Laboratory Apparatus: (a) 3-D schematic diagram of chamber and (b) Cross-sectional configuration.

For the first step, the soil was mixed with water to achieve target gravimetric moisture content of 15.5%. The prepared soil was then compacted for target density of 14.71 kN/m^3 from the foundation to 85 cm of the chamber. After compaction, slope was created with three gradients of 73.3° (L/H = 0.3), 59° (L/H = 0.6), and 45° (L/H = 1) [Figure 2(a)]. Then, GREW was constructed with the geotextiles and re-bar reinforcements. Specifically, the soil was compacted with the reinforcements in 17 layers (same target density of 14.71 kN/m^3) [Figure 2(b)]. 5 LVDTs were then installed on GREW with uniform spacing of 12 cm. Thereafter, 50 kPa load was applied on top of the soil. Three loads of 50 kPa, 100 kPa, and 250 kPa were cumulatively applied when the displacements were stabilized.

(a) original slope of 73.3° (b) Construction of GREW

Figure 2. Testing procedures: (a) original slope of 73.3°and (b) Constructing GREW in 17 layers.

3. RESULTS

Table 2 summarizes maximum horizontal displacements under 250 kPa and the maximum displacement locations, and Figure 3 compares horizontal displacements for original slopes, non-reinforced slopes, and GREWs at the three gradients (45°, 59°, 73.3°) under the three loads (50 kPa, 100 kPa, 250 kPa). As the loading and slope gradient increased, horizontal displacements toward the face increased, and maximum horizontal displacement was 36.9 cm at original slope of 73.3° under 250 kPa. Although surfaces of the original and non-reinforced slopes at 73.3° were slightly collapsed under 250 kPa, particularly at the original slope surface, no collapse failure was observed at GREWs. This is interpreted to reflect extensibility of the geotextiles and the type of facing, as described in the literature (Viswanadham and König, 2009). Locations of the maximum displacement varied depending on the slope gradient. The locations moved upward (e.g., from 490 mm to 730 mm), with decreases in the horizontal displacements, as slope gradient decreased from 73.3° to 45°. In other words, the decreased slope gradient (e.g., 45°) led to a decrease in shear stress, which was caused by gravitational force, resulting in an increase in shear strength of the slope.

Table 2. Summary of maximum horizontal displacements under 250 kPa and locations.

Slope Type	Slope Gradient (°)	Maximum Horizontal Displacement (mm)	Location (Distance from the Foundation) (mm)
Original Slope	73.3	36.9	490
	59	30.4	610
	45	24.5	730
Non-Reinforced Slope	73.3	29.6	490
	59	25.5	490
	45	20.5	730
GREW	73.3	12.5	490
	59	11.3	610
	45	6.7	730

For evaluating effects of geotextile lengths on horizontal displacements, additional tests were conducted with two different geotextile lengths: 14 cm (0.7L) and 10 cm (0.5L). Figure 4 and Table 3 show maximum horizontal displacements under 250 kPa at slope gradients of 45°, 59°, and 73.3° with four different geotextile lengths of 0 cm (0L), 10 cm (0.5L), 14 cm (0.7L), and 20 cm (1L). According to Christopher et al. (1990), horizontal displacement decreases by 50% when a length-to-height ratio of reinforcements increases from 0.5H to 0.7H. Similarly, in this study, the maximum displacements at the three gradients decreased by 33% when the geotextile length increased from 0.5L to 0.7L. Moreover, comparisons of 0L and 1L geotextiles demonstrate that maximum displacements decreased approximately by 60.3% with applying the geotextiles (i.e., from 0L to 1L) %. However, there was no critical length of the geotextile observed in this study. These findings indicate geotextiles were significantly effective to reduce the horizontal displacements due to increases in the cohesion and friction angle at interfaces between the soil and geotextile. This is also supportive of findings in Tuna and Altun (2012) that shear strength of geotextile-reinforced soils was not considerably reduced after peak strength, due to an increase in confinement effect.

Table 3. Summary of maximum horizontal displacements at three slope gradients with four geotextile lengths.

Geotextile Length	Slope Gradient (°)	Maximum Horizontal Displacement (mm)	Location (Distance from the Foundation) (mm)
0L	73.3	29.6	490
	59	25.5	490
	45	20.5	730
0.5L	73.3	23.5	490
	59	20.0	490
	45	14.5	730
0.7L	73.3	16.0	490
	59	13.7	490
	45	9.5	730
1L	73.3	12.5	490
	59	11.3	610
	45	6.7	730

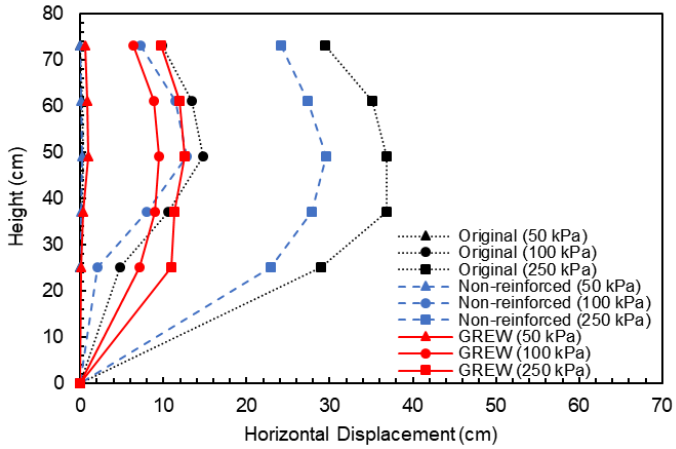

(a) slope gradient of 73.3°

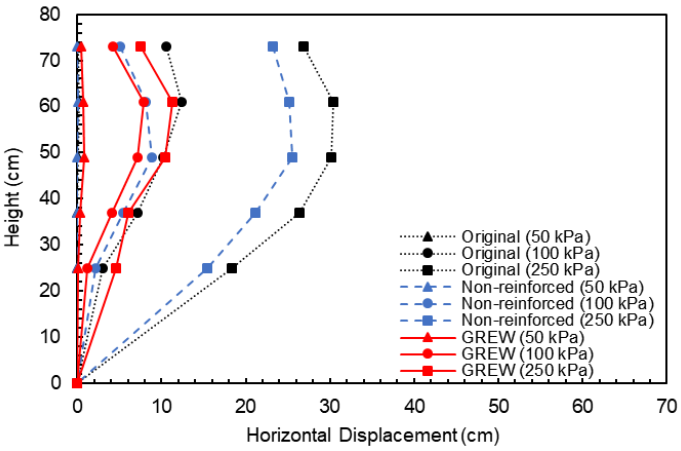

(b) slope gradient of 59°

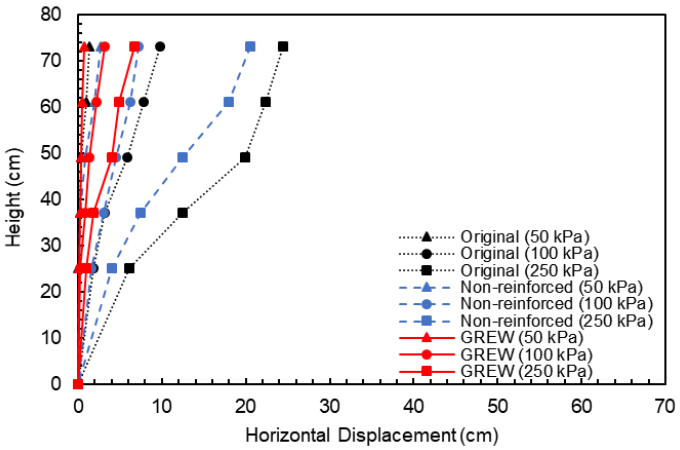

(c) slope gradient of 45°

Figure 3. Horizontal displacements under 50 kPa, 100 kPa, and 250 kPa at: (a) slope gradient of 73.3°, (b) slope gradient of 59°, and (c) slope gradient of 45°.

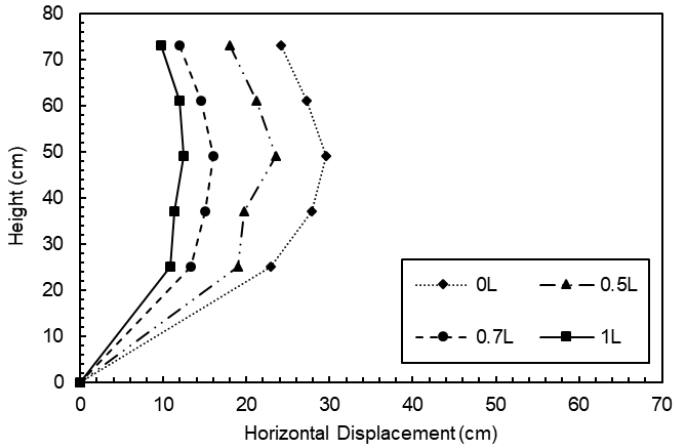

(a) slope gradient of 73.3°

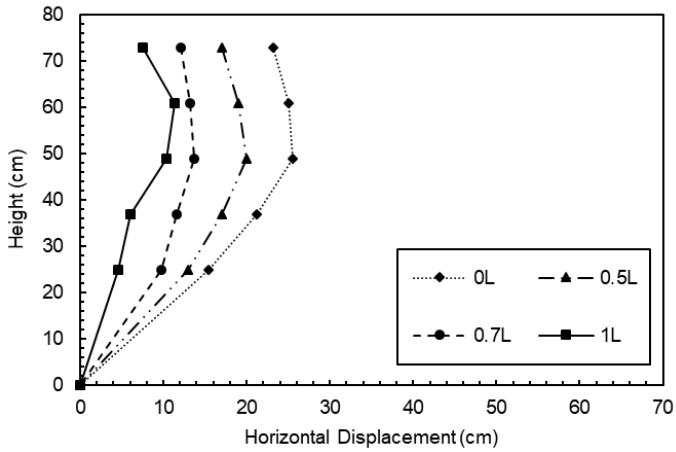

(b) slope gradient of 59°

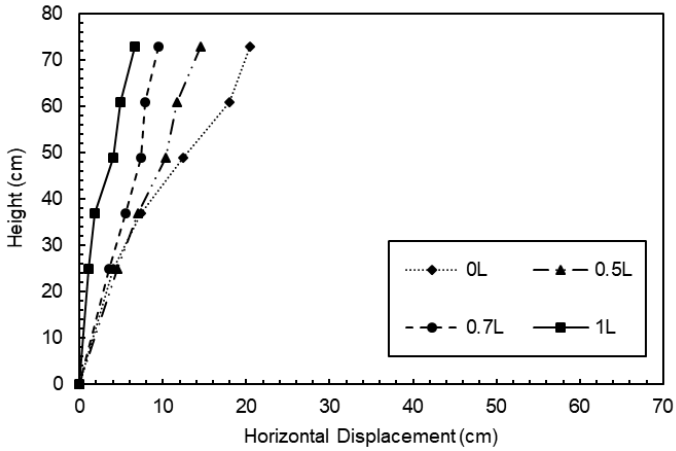

(c) slope gradient of 45°

Figure 4. Maximum horizontal displacements under 250 kPa with four geotextile lengths at: (a) slope gradient of 73.3°, (b) slope gradient of 59°, and (c) slope gradient of 45°.

4. SUMMARY AND CONCLUSIONS

In this study, behavior of GREW at three inclinations of 73.3°, 59°, and 45° was evaluated by laboratory tests. Horizontal displacements were measured using 5 LVDTs, which have 12 cm spacing, when applying three cumulative loads from 50 kPa to 250 kPa. The horizontal displacements were then compared to those of original and non-reinforced slopes. Furthermore, effect of the geotextile lengths on the horizontal displacements was investigated with four different geotextile lengths (0 cm, 10 cm, 14 cm, and 20 cm). Findings obtained from the experiments were as follows:

1) Horizontal displacements increased generally when slope gradient and load increased from 45° to 73.3° and 50 kPa to 250 kPa, respectively;
2) Locations of the maximum displacements moved upward as the gradient decreased;
3) Original and non-reinforced slopes at 73.3° were collapsed slightly under 250 kPa, but collapse was not observed in all GREW cases;
4) Maximum displacements decreased approximately by 60.3% when the geotextile length increased from 0 cm to 20 cm.

These findings indicate that slope stability may be increased with optimized slope inclination and geotextile length. These results provide empirical backgrounds for mechanistically sound and precise GREW design. Future research will be extended to numerical analysis to extensively validate and evaluate GREW behavior under various conditions, such as moisture content, soil density, and type and spacing of reinforcements.

ACKNOWLEDGEMENTS

This study was funded by Siwoo Construction Co, Ltd. (Seoul, South Korea). The experimental tests were conducted at Geotechnical Engineering Lab at the University of Seoul. Special thanks to Professor Song Lee for his advice.

REFERENCES

Al Hattamleh, O. and Muhunthan, B. (2006). Numerical procedures for deformation calculations in the reinforced soil walls, *Geotextiles and Geomembranes*, Elsevier, 24(1): 52–57.

Bakeer, R. M., Abdel-Rahman, A. H., and Napolitano, P. J. (1998). Geotextile friction mobilization during field pullout test, *Geotextiles and Geomembranes*, Elsevier, 16(2): 73–85.

Benjamim, C. V. S., Bueno, B. S., and Zornberg, J. G. (2007). Field monitoring evaluation of geotextile-reinforced soil-retaining walls, *Geosynthetics International*, ICE Publishing, 14(2): 100–118.

Hatami, K. and Bathurst, R. (2005). Development and verification of a numerical model for the analysis of geosynthetic-reinforced soil segmental walls under working stress conditions, Canadian Geotechnical Journal, NRC Research Press, 42(4): 1066–1085.

Chen, H.T., Hung, W.Y., Chang, C.C., Chen, Y.J., Lee, C.J. (2007). Centrifuge modeling test of a geotextile-reinforced wall with a very wet clayey backfill, *Geotextiles and Geomembranes*, Elsevier, 25(6): 346–359.

Christopher, B. R., Gill, S. A., Giroud, J.-P., Juran, I., Mitchell, J. K., Schlosser, F., and Dunnicliff, J. (1990). Reinforced soil structures Vol. 1, Design and construction guidelines. *FHWA Rep. No. FHWARD-89-043*, Federal Highway Administration, Washington, D.C., USA.

Claybourn, A. F. and Wu, J. T. H. (1993). Geosynthetic-reinforced soil wall design, *Geotextiles and Geomembranes*, Elsevier, 12(8): 707–724.

Juran, I. and Christopher, B. (1989). Laboratory model study on geosynthetic reinforced soil retaining walls, *Journal of Geotechnical Engineering*, ASCE, 115(7).

Lee, K. M. and Manjunath, V. R. (2000). Experimental and numerical studies of geosynthetic-reinforced sand slopes loaded with a footing, Canadian Geotechnical Journal, NRC Research Press, 37(4): 828–842.

Leshchinsky, D. (1985). Design manual for geotextile-retained earth walls, *Research Report No. CE-85-51*, Department of Civil Engineering, University of Delaware, Newark, DE, USA.

Porbaha, A. and Goodings, D. J. (1996). Centrifuge Modeling of Geotextile-Reinforced Cohesive Soil Retaining Walls, *Journal of Geotechnical Engineering*, ASCE, 122(10): 840–848.

Portelinha, F. H. M., Bueno, B. S., and Zornberg, J. G. (2012). Performance of geotextile reinforced soil wall in unsaturated poorly draining backfill soil conditions, *5th European Geosynthetics Congress*, IGS, Valencia, Spain, 5: 455–465.

Portelinha, F. H. M., Bueno, B. S., and Zornberg, J. G. (2013). Performance of nonwoven geotextile-reinforced walls under wetting conditions: laboratory and field investigations, *Geosynthetics International*, ICE Publishing, 20(2): 90–104.

Portelinha, F. H. M., Zornberg, J. G., and Pimentel, V. (2014). Field performance of retaining walls reinforced with woven and nonwoven geotextiles, *Geosynthetics International*, ICE Publishing, 21(4): 270–284.

Rowe, R. K. and Skinner, G. D. (2001). Numerical analysis of geosynthetic reinforced retaining wall constructed on a layered soil foundation, *Geotextiles and Geomembranes*, Elsevier, 19(7): 387–412.

Tuna, S. C. and Altun, S. (2012). Mechanical behavior of sand-geotextile interface, *Scientia Iranica*, Sharif University of Technology, 19(4): 1044–1051.

Viswanadham, B.V.S. and König, D. (2009). Centrifuge modeling of geotextile-reinforced slopes subjected to differential settlements, *Geotextiles and Geomembranes*, Elsevier, 27(2): 77–88.